THE JOURNAL OF BIOLOGICAL CHEMISTRY VOL. 287, NO. 49, pp. 41032–41043, November 30, 2012

The MicroRNA miR-199a-5p Down-regulation Switches on Wound Angiogenesis by Derepressing the *v-ets* Erythroblastosis Virus E26 Oncogene Homolog 1-Matrix Metalloproteinase-1 Pathway*[S]

Received for publication, August 28, 2012, and October 2, 2012 Published, JBC Papers in Press, October 11, 2012, DOI 10.1074/jbc.M112.413294

Yuk Cheung Chan, Sashwati Roy, Yue Huang, Savita Khanna, and Chandan K. Sen[1]

From the Department of Surgery, Davis Heart and Lung Research Institute, The Ohio State University Medical Center, Columbus, Ohio 43210

Background: The role of miR-199a-5p in angiogenesis remains unclear.
Results: miR-199a-5p exerts angiostatic effects by targeting Ets-1-MMP1 pathway and is down-regulated in skin wound healing.
Conclusion: Down-regulation of miR-199a-5p switches on wound angiogenesis through derepressing of Ets-1-MMP1 pathway.
Significance: This investigation provides novel mechanistic insight explaining miR-dependent regulation of wound angiogenesis and the foundation of developing therapeutic intervention in treating chronic nonhealing wounds.

miR-199a-5p plays a critical role in controlling cardiomyocyte survival. However, its significance in endothelial cell biology remains ambiguous. Here, we report the first evidence that miR-199a-5p negatively regulates angiogenic responses by directly targeting v-*ets* erythroblastosis virus E26 oncogene homolog 1 (Ets-1). Induction of miR-199a-5p in human dermal microvascular endothelial cells (HMECs) blocked angiogenic response in Matrigel® culture, whereas miR-199a-5p-deprived cells exhibited enhanced angiogenesis *in vitro*. Bioinformatics prediction and miR target reporter assay recognized Ets-1 as a novel direct target of miR-199a-5p. Delivery of miR-199a-5p blocked Ets-1 expression in HMECs, whereas knockdown endogenous miR-199a-5p induced Ets-1 expression. Matrix metalloproteinase 1 (MMP-1), one of the Ets-1 downstream mediators, was negatively regulated by miR-199a-5p. Overexpression of Ets-1 not only rescued miR-199a-5p-dependent anti-angiogenic effects but also reversed miR-199a-5p-induced loss of MMP-1 expression. Similarly, Ets-1 knockdown blunted angiogenic response and induction of MMP-1 in miR-199a-5p-deprived HMECs. Examination of cutaneous wound dermal tissue revealed a significant down-regulation of miR-199a-5p expression, which was associated with induction of Ets-1 and MMP-1. Mice carrying homozygous deletions in the Ets-1 gene exhibited blunted wound blood flow and reduced abundance of endothelial cells. Impaired wound angiogenesis was associated with compromised wound closure, insufficient granulation tissue formation, and blunted induction of MMP-1. Thus, down-regulation of miR-199a-5p is involved in the induction of wound angiogenesis through derepressing of the Ets-1-MMP1 pathway.

Angiogenesis, sprouting of pre-existing blood vessels, is one of the major biological responses supporting both cutaneous wound healing and tumorogenesis. Emerging evidence has revealed that microRNAs (miRs)[2] play a critical role in regulation of angiogenesis (1, 2). These small RNA exert substantial gene regulatory effects by a number of ways including physical interaction with the 3′-UTR of mRNA, hindering translation or leading to transcript degradation. Our group and others have characterized the significance of specific miRs in modulating the angiogenic response. miR-210, for example, supports angiogenesis by targeting angiostatic proteins ephrin-A3 and protein-tyrosine phosphatase 1B (1). miR-200b, a hypoxia-repressible miR (3), negatively regulates angiogenic response by silencing vascular endothelial growth factor (4), GATA-binding protein 2 (5), and vascular endothelial growth factor receptor 2 (5).

miR-199a-5p is a multifaceted miR that regulates cell survival during ischemia-reperfusion injury (6–8). It is expressed in a variety of organs including the brain (6), liver (9), stomach (10), ovarian tissue (11, 12), testicular tissue (13), and the cardiovascular system, such as in cardiomyocytes (7, 8) and endothelial cells (14, 15). Recent evidence revealed that miR-199a-5p plays a critical role in attenuating cell migration and in limiting cancer cell metastasis by targeting receptor tyrosine kinase Discoidin domain receptor-1 (9), Axl (16), and anti-adhesive transmembrane glycoprotein podocalyxin-like protein 1 (13). We hypothesized that miR-199a-5p exerts angiostatic effects on endothelial cells. In this report, we provide the first evidence that inhibition of endogenous miR-199a-5p in endothelial cells supports angiogenesis, and first characterized v-*ets* erythroblastosis virus E26 oncogene homolog 1 (Ets-1) as a *bona fide* miR-199a-5p target. We found that matrix metalloproteinase 1

* This work was supported, in whole or in part, by National Institutes of Health Grants GM 077185 and GM069589 (to C. K. S.) and DK076566 (to S. R.).
[S] This article contains supplemental Table S1 and Figs. S1–S7.
[1] To whom correspondence should be addressed: Ohio State Univ., 473 West 12th Ave., Columbus, OH 43210. Tel.: 614-247-7658; Fax: 614-247-7818; E-mail: chandan.sen@osumc.edu.

[2] The abbreviations used are: miR, microRNA; Ets-1, v-*ets* erythroblastosis virus E26 oncogene homolog 1; HMEC, human microvascular endothelial cell; HIF, hypoxia-inducing factor; LCM, laser capture microdissection; MMP-1, matrix metalloproteinase 1.

(MMP-1) is the key downstream mediator of the miR-199a-5p-Ets-1 pathway. Down-regulation of miR-199a-5p enables cutaneous wound angiogenesis via derepression of Ets-1 and subsequent induction of MMP-1.

EXPERIMENTAL PROCEDURES

Cell and Cell Culture—Human dermal microvascular endothelial cells (HMECs) were grown in MCDB-131 medium supplemented with 10% FBS, 10 mM L-glutamine, 100 IU/ml penicillin, and 0.1 mg/ml streptomycin as described previously (2, 3, 5). Primary adult human dermal microvascular endothelial cells were cultured in EBM-2 medium (Lonza, Basel, Switzerland) supplemented with EGM-2MV single quotes as described by the manufacturer. HEK-293 cells were maintained with high glucose DMEM supplemented with 10% FBS and 100 IU/ml penicillin, 0.1 mg/ml streptomycin. All of the cells were cultured in standard culture conditions (at 37 °C with 20% O_2 and 5% CO_2). The cells were seeded in a 12-well plate at a density of 0.12×10^6 cells/well 24 h before treatment. Delivery of small RNAs was achieved using DharmaFECTTM 1 transfection reagent (Dharmacon RNA Technologies, Denver, CO). miR-199a-5p mimic (50 nM), miR-199a-5p inhibitor (100 nM), or siRNA smart pool for human Ets-1 or MMP-1 (100 nM) were obtained from Dharmacon RNA Technologies. Unless specific, the cells were lysed after 72 h (HMECs and HEK-293) or 48 h (primary endothelial cells) of transfection and RNA/protein were collected for gene expression study. For Ets-1 overexpression studies, expressing plasmid encoding Ets-1 (Ets-1 pcDNA), a generous gift from Dr. Michael C. Ostrowski (The Ohio State University, Columbus, OH) (17) (1 μg/well), was delivered to the endothelial cells using Lipofectamine TM LTX/plus reagent as described previously (3). Two days after the plasmid delivery, the cells were subjected to miR-199a-5p mimic (or control mimic) delivery as described above for another 48 h for Matrigel® analysis, and RNA/protein extraction. For miR-199a-5p inhibitor-Ets-1 siRNA co-transfection study, both miR-199a-5p inhibitor and Ets-1 siRNA (or control siRNA) were mixed together and incubated with DharmaFECTTM 1 transfection reagent. For 72 h, the gene-liposome complex was delivered to endothelial cells that were subjected to *in vitro* angiogenesis studies or for RNA/protein extraction.

Mice and Secondary Intention Excisional Murine Dermal Wound Model—Male C57BL/6 mice (age, 8–10 weeks old) were obtained from Harlan Laboratory. The Ets-1-deficient mice (129/Sv × C57BL/6 × FVB/N) were kindly provided by Dr. Michael C. Ostrowski. Genotyping was performed with DNA from tail biopsies by PCR using specific primers (supplemental Table S1) with the following protocol: 94 °C for 45 s, 58 °C for 45 s, and 72 °C for 1 min (40 cycles). Two or four 6-mm diameter full thickness excisional wounds were developed on the dorsal skin of mice with a 6-mm disposable biopsy punch. A surgical splinted wound model was employed for the wound closure study, histological analysis, and collagen deposition assessment as described previously (18). Briefly, a donut-shaped splint with a 8-mm inner diameter was created from a 0.5-mm-thick silicone sheet (Grace Bio-Laboratories, Bend, OR) and placed such that the wound was centered within the splint. To fix the splint to the skin, an immediate bonding adhesive was used, followed by interrupted 5–0 nylon sutures (Ethicon, Inc., Somerville, NJ) to maintain position. All of the animal studies were performed in accordance with protocols approved by the Laboratory Animal Care and Use Committee of the Ohio State University. During the wounding procedure, the mice were anesthetized by low dose isoflurane inhalation for 5–10 min/standard recommendation. Each wound was digitally photographed at the time point indicated. Wound size was calculated by the software Image J. The animals were sacrificed at the indicated postwounding time point, and wound tissues were harvested (as frozen, in optimal cutting temperature compound or fixed in buffered formalin) for further analysis.

RNA Isolation and Quantitative Real Time PCR—The miRVana miRNA isolation kit was employed to extract total RNA from tissue and cells according to the manufacturer's protocol (Ambion). miR expression was determined by miR TaqMan assays and TaqMan microRNA reverse transcription kit, followed by quantitative real time PCR using Universal PCR Master Mix (Applied Biosystems) (3, 5). For mRNA expression studies, total cDNA synthesis was achieved by a SuperScript™ III first strand synthesis system (Applied Biosystems). The transcription levels of Ets-1, MMP-1, MMP-3, and MMP-9 were assessed by real time PCR using SYBR green-I (Invitrogen) as described previously (3, 5). The sequences of primers are shown in supplemental Table S1.

miR Target Reporter Luciferase Assay—pLu-wild type Ets1–3′-UTR plasmid or construct carrying the mutation of the predicted miR-199a-5p binding site in Ets1–3′-UTR (100 ng) (Signosis, Sunnyvale, CA) was delivered to HEK-293 cells using Lipofectamine™ LTX/plus reagent (Invitrogen) according to the manufacturer's protocol. The constructs were designed based on the sequence of miR-199a-5p binding sites and a total of 300 bp (starting from positions 2551–2850 of Ets-1 3′-UTR) was cloned in the 3′-UTR of constitutively active firefly luciferase construct. Mutation was made in the predicted miR-199a-5p binding site (from ACACUGG to UGUGACC, position 2708–2714 of Ets-1 3′-UTR). Constitutively active *Renilla* luciferase plasmid (10 ng) was delivered to cells for normalization. The cell lysates were assayed with dual luciferase reporter assay kit (Promega, Madison, WI). The data are presented as ratio of firefly to *Renilla* luciferase activity as described previously (3, 5).

Matrigel® Assay—In vitro angiogenesis assay were assessed by tube formation ability on Matrigel® culture as described previously (3, 5). Endothelial cells were seeded on Matrigel® precoated plate at a density of 5×10^4 cells/well. The angiogenic ability was assessed 8 h (HMECs) or 24 h (primary endothelial cells) after plating on Matrigel®, and the tube length was measured using the software AxioVision Rel 4.6 (Zeiss) (3, 5).

Cell Migration Assay—Cell migration was determined using culture insert (Ibidi, Verona, WI) according to the manufacturer's instruction. Briefly, the cells were seeded at the confluent monolayer on the chambers of the culture insert. After seeding for 1 h, the insert was removed, and the cells were allowed to migrate. Cell migratory distance was measured 4 h after removal of insert using AxioVision Rel 4.6 software (Zeiss).

Cell Proliferation—Transfected cells were seeded in 96-well plate, and cell proliferation was determined by the CyQUANT®

cell proliferation assays (Invitrogen) as described previously (19).

Western Blots—Western blot was performed using antibodies against Ets-1 (Santa Cruz Biotechnology, Santa Cruz, CA) (3) and mouse MMP-1 (Abbiotec, San Diego, CA) (20). Briefly, proteins were extracted from cells or mouse tissues with lysis buffer consisting of 10 mM Tris, pH 7.4, 150 mM NaCl, 1% Triton X-100, 1% deoxycholic acid, 0.1% SDS, and 5 mM EDTA. Cell lysate or tissue homogenate was resolved in SDS-PAGE and transblotted to PVDF membrane (GE Healthcare), followed by blocking with 10% skim milk and incubation with primary antibody against Ets-1 (1:3,000), MMP-1 (1:1,000) or β-actin (Sigma; 1: 10,000) (as loading control) overnight at 4 °C. The signal was visualized using corresponding HRP-conjugated secondary antibody (GE Healthcare; 1:3,000) and ECL Plus™ Western blotting detection reagents (GE Healthcare).

Immunohistochemistry and Immunocytochemistry—Immunohistochemistry of Ets-1 and CD31 was performed on cryosections of wound sample using specific antibodies as described previously (5). The wound tissue isolated was embedded in optimal cutting temperature compound and cryosectioned at 10 μm thick. Tissue sections were fixed with acetone, blocked with 10% normal goat serum, followed by incubation with antibodies against endothelial marker CD31 (BD Bioscience, San Jose, CA; 1:400) and Ets-1 (1:500) overnight at 4 °C. Signal was visualized by reaction with fluorescence-tagged secondary antibodies (FITC-tagged α-rat, 1:200; Alexa 568-tagged α-rabbit, 1:200) (Invitrogen; 1:200), counterstained with DAPI (Invitrogen; 1:10,000). For immunocytochemistry, the cells were fixed with 4% paraformaldehyde, permeabilized with 0.1% Triton X-100, blocked, and incubated with primary antibody against Ets-1 (1: 500) or MMP-1 (Abcam, Cambridge, MA; 1:50) overnight at 4 °C. Signal was visualized using Alexa Fluor® 488 dye-conjugated antibody against rabbit, counterstained with rhodamine phalloidin (Invitrogen; 1:250), and DAPI. The images were captured by microscope, and quantification of fluorescent intensity of image was achieved by the software AxioVision Rel 4.6 (Carl Zeiss Microimaging).

Histological Analyses—Hematoxylin-eosin and Masson's trichrome staining were performed as described by our group previously (21). Briefly, tissue was collected and fixed in 10% buffered formalin solution for 2 weeks, after which they were processed for dehydration and paraffin embedding. Paraffin-embedded tissue was sectioned at 5 μm and processed for hematoxylin-eosin and Masson's trichrome staining.

Laser Capture Microdissection (LCM)—LCM was performed using the laser microdissection system from PALM Technologies (Bernreid, Germany) containing a PALM MicroBeam and RoboStage for high throughput sample collection and a PALM RoboMover (PALM Robo software, version 2.2) as described previously (5). For immunofluorescence-directed LCM, blood vessels were stained with CD31 antibody (1:25), FITC-conjugated secondary antibody (1:200), and subsequently visualized using fluorescent lamp. For dermal LCM, dermal fraction was identified based on the histology after hematoxylin staining. Endothelial or dermal tissue elements were isolated and captured under a 20× ocular lens, using cut elements. Approximately 150,000 μm^2 of tissue area was captured into lysis extraction buffer, and the extract was then held at −80 °C for extraction process (5).

Laser Doppler—Dermal blood flow was analyzed by laser Doppler imager as described previously (5). The MoorLDI-Mark 2 laser Doppler blood perfusion imager (resolution, 256 × 256 pixels; visible red laser beam at 633 nm) was used for mapping tissue blood flow under isofuran anesthetization.

Statistical Analyses—The data reported represent the means ± S.E. Difference between two means was tested by Student *t* test, whereas one-way analysis of variance analysis was employed to compare three groups or more. $p < 0.05$ was considered statistically significant.

RESULTS

miR-199a-5p Is Angiostatic in HMECs—To determine the role of miR-199a-5p specifically on the angiogenic response of endothelial cells *in vitro*, miR-199a-5p mimic was transiently delivered to HMECs, and Matrigel® tube formation was analyzed. Delivery of miR-199a-5p to the endothelial cells not only led to significant accumulation of miR-199a-5p (Fig. 1*A*) but also exerted potent angiostatic effects (80% down-regulation compared with control) (Fig. 1*C*). Treatment of miR-199a-5p hairpin inhibitor blocked the endogenous expression of miR-199a-5p (Fig. 1*B*). Down-regulation of miR-199a-5p was accompanied by significant induction of tube formation ability by 40% in Matrigel® culture (Fig. 1*D*). To investigate whether miR-199a-5p exerts general angiostatic effect on endothelial cells, we examine the effect of miR-199a-5p mimic or inhibitor on primary adult human dermal microvascular endothelial cells. Delivery of miR-199a-5p mimic to primary endothelial cells significantly attenuated the tube formation ability on Matrigel® (supplemental Fig. S1, *A* and *B*), which was comparable with that on HMECs. Similarly, depletion of miR-199a-5p in primary endothelial cells significantly resulted in enhancement of angiogenic response. (supplemental Fig. S1, *C* and *D*). Consistent with the Matrigel® study, delivery of miR-199a-5p mitigates endothelial cell migration (supplemental Fig. S2*A*). miR-199a-5p does not exert any effect on endothelial cell proliferation (supplemental Fig. S2*B*).

miR-199a-5p Directly Targets Ets-1 by Interacting with the 3′ UTR—To delineate the mechanisms underlying the angiostatic effect, bioinformatics analyses were performed to investigate the possible direct target using algorithms including Targetscan (22), Pictar (23), MiRanda (22), and miRDB (24). *In silico* analysis revealed that Ets-1 3′-UTR contains a highly conserved binding site at positions 2708–2714 for miR-199a-5p (Fig. 2*A* and supplemental Fig. S3*A*). To experimentally validate the possible interaction between miR-199a-5p and Ets-1 3′-UTR, miR target reporter luciferase assay was performed using construct pLuc-Ets1–3′-UTR plasmid (supplemental Fig. S3*B*). Delivery of miR-199a-5p mimic resulted in 35% reduction of luciferase activity compared with control mimic delivered cells (Fig. 2*B*). To test whether the binding was specific to the predicted binding site, similar reporter assay was performed using the construct carrying the mutation of the predicted site (supplemental Fig. S3*B*). Mutation of the predicted binding site significantly abolished miR-199a-5p-associated inhibition of luciferase activity, suggesting that miR-199a-5p specifically

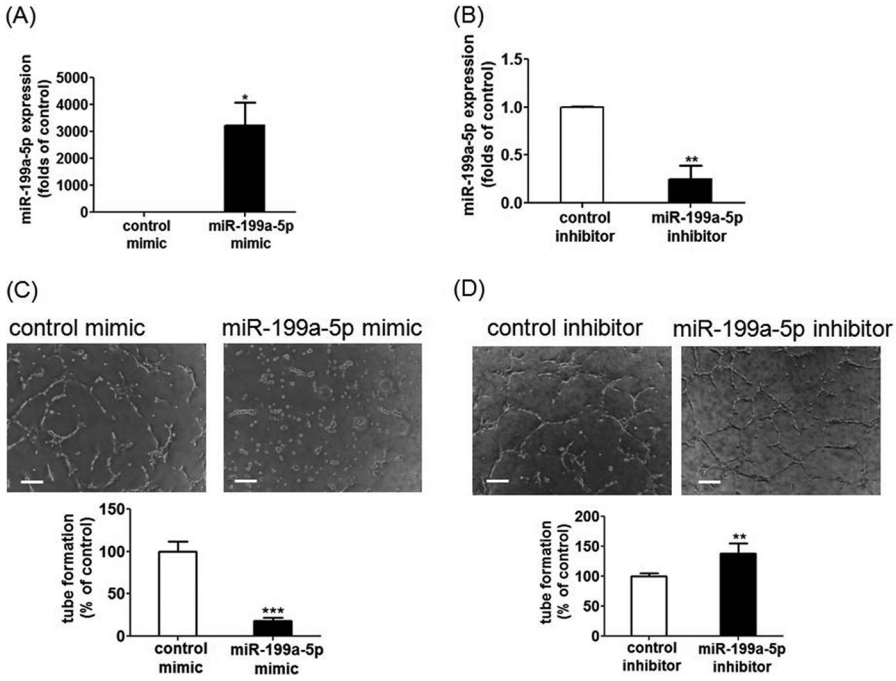

FIGURE 1. **miR-199a-5p induces angiostatic effects in HMECs.** *A* and *B*, quantitative real time PCR analysis of miR-199a-5p expression after delivery of miR-199a-5p mimic (*A*) or miR-199a-5p inhibitor (*B*). *C* and *D*, HMECs were subjected to Matrigel® culture after transfection of miR-199a-5p mimic (*C*) or miR-199a-5p inhibitor (*D*). Images of tube formation were visualized and captured by phase contrast microscopy. Representative images are shown from at least three independent experiments. *Scale bar*, 200 μm. Quantification of length of tube formation (percentage of control) of miR-199a-5p mimic or miR-199a-5p inhibitor-delivered cells is shown. The results are the means ± S.E. *, $p < 0.05$; **, $p < 0.01$; ***, $p < 0.001$ compared with control.

binds to the predicted binding site in Ets-1 3′-UTR exerting translational repression (Fig. 2*B*). Western blot analysis suggested that miR-199a-5p negatively regulates Ets-1 expression in endothelial cells. Delivery of miR-199a-5p blunted Ets-1 expression in HMECs by 65% (Fig. 2*C*). On the other hand, repression of endogenous miR-199a-5p significantly induced Ets-1 expression by 2.5-folds (Fig. 2*D*). These observations were consistent with the findings from immunocytochemistry. Ets-1 protein expression in both cytosolic (signal co-localized with Phalloidin) and nuclear (signal co-localized with DAPI) compartment of endothelial cells is down-regulated by exogenous miR-199a-5p (Fig. 2*E*). Similarly, primary endothelial cells with miR-199a-5p mimic delivered exhibited attenuated Ets-1 expression (supplemental Fig. S1*E*). It was thus identified that Ets-1 is a *bona fide* target of miR-199a-5p in human dermal microvascular endothelial cells.

miR-199a-5p Blocked the Expression of Ets-1 Downstream Mediator MMP-1—Ets-1 is a multifaceted transcription factor controlling the expression of genes essential for cell migration and motility. In particular, angiogenesis requires modulation of extracellular matrix facilitating endothelial migration. Previous investigations revealed that MMP-1 is one of the major Ets-1 downstream mediators enabling endothelial migration (25). Delivery of siRNA against Ets-1 or MMP-1 alone recapitulated the angiostatic effect of miR-199a-5p (supplemental Fig. S4). Knocking down Ets-1 in HMECs significantly inhibited MMP-1 mRNA expression, exerting 75% repression (Fig. 3*A*). Intriguingly, delivery of synthetic miR-199a-5p suppressed MMP-1 expression mimicking the effect of Ets-1 knockdown (Fig. 3*B*). Inhibition of endogenous miR-199a-5p expression induced MMP-1 expression by 45% in endothelial cells (Fig. 3*C*). These results were in good agreement with the MMP-1 protein analysis using immunocytochemistry (supplemental Fig. S5). Primary dermal microvascular endothelial cells with miR-199a-5p mimic delivery exhibited reduced MMP-1 expression (supplemental Fig. S1*F*). Other Ets-1-associated MMPs such as MMP-3 and MMP-9 were not involved in miR-199a-5p-dependent angiostatic effects (supplemental Fig. S6).

Ets-1 Serves as a Downstream Mediator of miR-199a-5p-dependent Angiogenic Control—To test the hypothesis that Ets-1 serves as a downstream mediator of miR-199a-5p signaling in endothelial cells, HMECs were subjected to Ets-1 overexpression followed by delivery of miR-199a-5p mimic. Overexpression of Ets-1 not only significantly induced Ets-1 expression (supplemental Fig. S7*A*) but also rescued the angiostatic effects of miR-199a-5p mimic (Fig. 4*A*). On the other hand, treatment of Ets-1 siRNA inhibited the expression of Ets-1 in the presence of miR-199a-5p inhibitor (supplemental Fig. S7*B*) and blunted the pro-angiogenic response induced by anti-miR-199a-5p treatment (Fig. 4*B*). Similarly, miR-199a-5p-associated down-regulation of MMP-1 was reversed by Ets-1 overexpression (Fig. 4*C*). Delivery of Ets-1 siRNA to HMECs blunted miR-199a-5p inhibitor-dependent induction of MMP-1 (Fig. 4*D*). These data suggest that Ets-1 serves as a downstream mediator of miR-199a-5p-dependent angiostatic control.

Murine Cutaneous Wound Edge Tissue Exhibited Decreased miR-199a-5p Expression, Ets-1 Induction, and Up-regulation of MMP-1—To connect the aforementioned observations to *in vivo* angiogenesis, we asked whether the miR-199a-5p-Ets-1-MMP-1 pathway takes place during postnatal angiogenesis such as during cutaneous wound healing. Our group previously reported that the miR-dependent angiogenic signals emerge

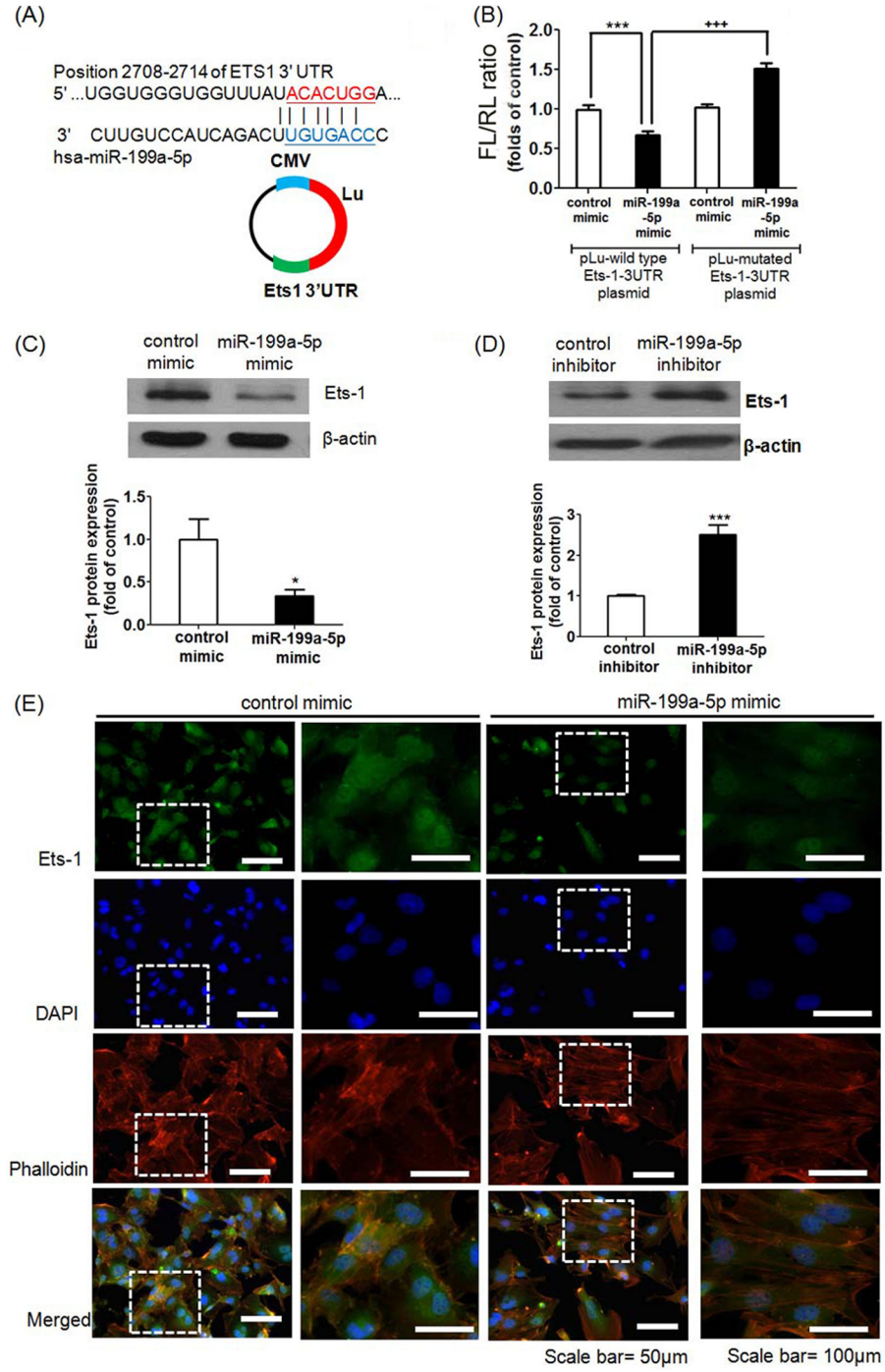

FIGURE 2. **Ets-1 serves as a *bona fide* miR-199a-5p target.** *A*, *in silico* study revealing a possible binding site in Ets-1 3′-UTR (at positions 2708–2714) for miR-199a-5p as predicted by Targetscan, Pictar, MiRanda, and miRDB. *B*, miR target reporter luciferase assay after miR-199a-5p mimic delivery in HEK-293 cells using wild type pLu-wild type Ets-1–3UTR plasmid or pLu-mutated Ets-1–3UTR plasmid. *Open bars* and *solid bars* represent control mimic and miR-199a-5p mimic delivered cells, respectively. The results were normalized with data obtained from assay with *Renilla* luciferase. *C* and *D*, Western blot analysis of Ets-1 protein expression in miR-199a-5p mimic delivered (*C*) or depleted (*D*) HMECs. β-Actin serves a loading control. Representative blots from three independent experiments and quantification of band intensity relative to control are presented. *E*, representative images showing Ets-1 protein expression (*green*) after miR-199a-5p mimic delivery from three independent experiments. Nuclear counterstain with DAPI (*blue*), actin staining with phalloidin (*red*), and the corresponding merged image are shown in the *bottom panels*. The results are the means ± S.E. ***, $p < 0.001$; *, $p < 0.05$ compared with corresponding control; +++, $p < 0.001$ compared with pLu-wild type Ets-1–3′-UTR plasmid transfected cells.

during inflammatory phase (5). We thus studied the expression level of miR-199a-5p day 3 postwounding in the excisional cutanous wound model. Data from dermal miR expression studies revealed a down-regulation of miR-199a-5p in response to wounding compared with intact skin in day 3 (Fig. 5*A*). These data are further supported by the real time PCR analysis of LCM endothelial tissue element from both skin and day 3 wound edge tissue, indicating that the expression of endothelial miR-199a-5p is down-regulated in response to wounding (Fig. 5*B*). The repression of miR-199a-5p was negatively associated with

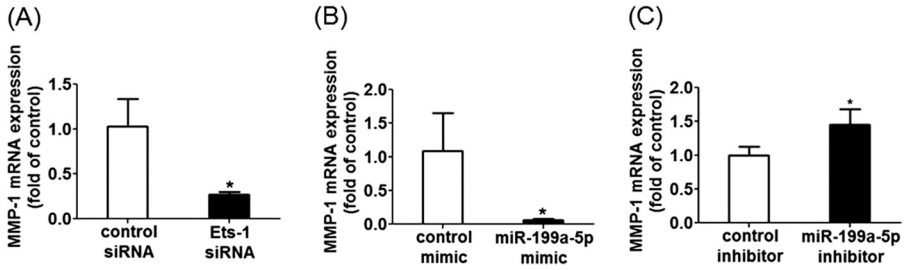

FIGURE 3. **Expression of MMP-1 in Ets-1 knock-down, miR-199a-5p mimic delivered and miR-199a-5p depleted HMECs.** Real time PCR analysis of MMP-1 expression after transfection of Ets-1 siRNA (*A*), miR-199a-5p mimic (*B*), or miR-199a-5p inhibitor (*C*) is shown. The results are the means ± S.E. *, $p < 0.05$ compared with corresponding control.

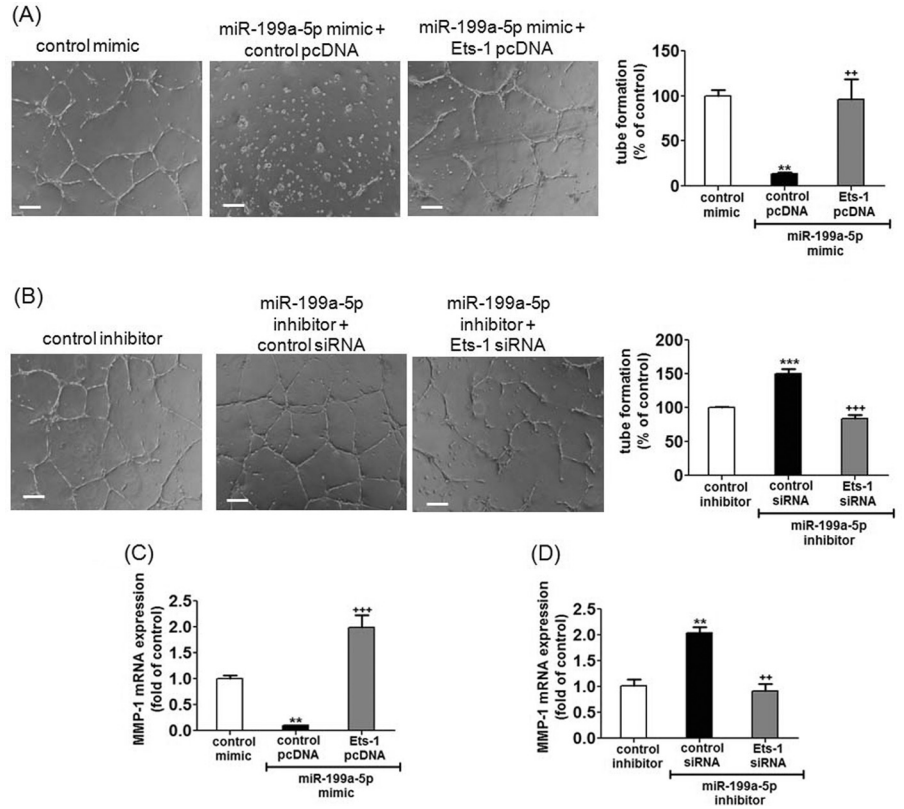

FIGURE 4. **Ets-1 overexpression or knockdown reversed miR-199a-5p-induced angiogenic control and its associated regulation of MMP-1 gene expression.** *A* and *B*, Matrigel® tube formation visualized by phase contrast microscopy at 8 h after delivery of control or miR-199a-5p mimic in the presence or absence of Ets-1 pcDNA (*A*) or control or miR-199a-5p inhibitor in the presence or absence of Ets-1 siRNA (*B*). Representative images are shown from three independent experiments. *Scale bar*, 200 μm. The *bar graphs* indicate quantification of length of tube formation (percentage of control). *C* and *D*, real time PCR analysis of MMP-1 expression after delivery of control or miR-199a-5p mimic in the presence or absence of Ets-1 pcDNA (*C*) or control or miR-199a-5p inhibitor in the presence or absence of Ets-1 siRNA (*D*). The results are the means ± S.E. **, $p < 0.01$ compared with control mimic/inhibitor; +++, $p < 0.001$; ++, $p < 0.01$ compared with miR-199a-5p mimic + pcDNA/miR-199a-5p + control siRNA.

the expression of Ets-1 and MMP-1. Wounding significantly induced endothelial Ets-1 expression in day 3 as evidenced from double-immunostaining (Fig. 5, *C* and *D*). The induction of Ets-1 was sustained until day 7 postwounding. Western blot analyses demonstrated that MMP-1 protein expression was significantly up-regulated in day 7 postwounding (Fig. 5*E*).

Loss of Ets-1 Impaired Wound Closure, Wound Angiogenesis, and Wound-induced MMP-1 Expression—To test the significance of Ets-1 in wound angiogenesis, we studied wound closure and wound angiogenesis in mice carrying homozygous deletions in the Ets-1 gene (Ets-$1^{-/-}$) (Fig. 6*A*). Genetic deletion of Ets-1 revealed significant reduction of Ets-1 protein expression in the skin tissue compared with their heterozygous (Ets-$1^{+/-}$) and wild type (Ets-$1^{+/+}$) littermates (Fig. 6*B*). Ets-$1^{-/-}$ mice exhibited compromised wound closure response (Fig. 6*C*). Consistent with this finding, histological analysis using hematoxylin-eosin (Fig. 7*A*) and Masson trichrome staining (Fig. 7*B*) showed significant impairment in re-epithelialization and collagen deposition in the wound edge tissue from Ets-$1^{-/-}$ mice. Interestingly, Ets-$1^{-/-}$ mice exhibited lower wound site blood flow as evidenced by laser Doppler analysis (Fig. 8*A*). This observation is in good agreement with the analysis of endothelial cell abundance using immunohistochemistry (Fig. 8*B*). Wound edge tissue from Ets-$1^{-/-}$ mice exhibited significant loss (by 65%) of endothelial cells compared with that in Ets-$1^{+/-}$ and Ets-$1^{+/+}$ mice. Such compromised angiogenic response was associated with blunting of wound-induced MMP-1 expression (Fig. 8*C*).

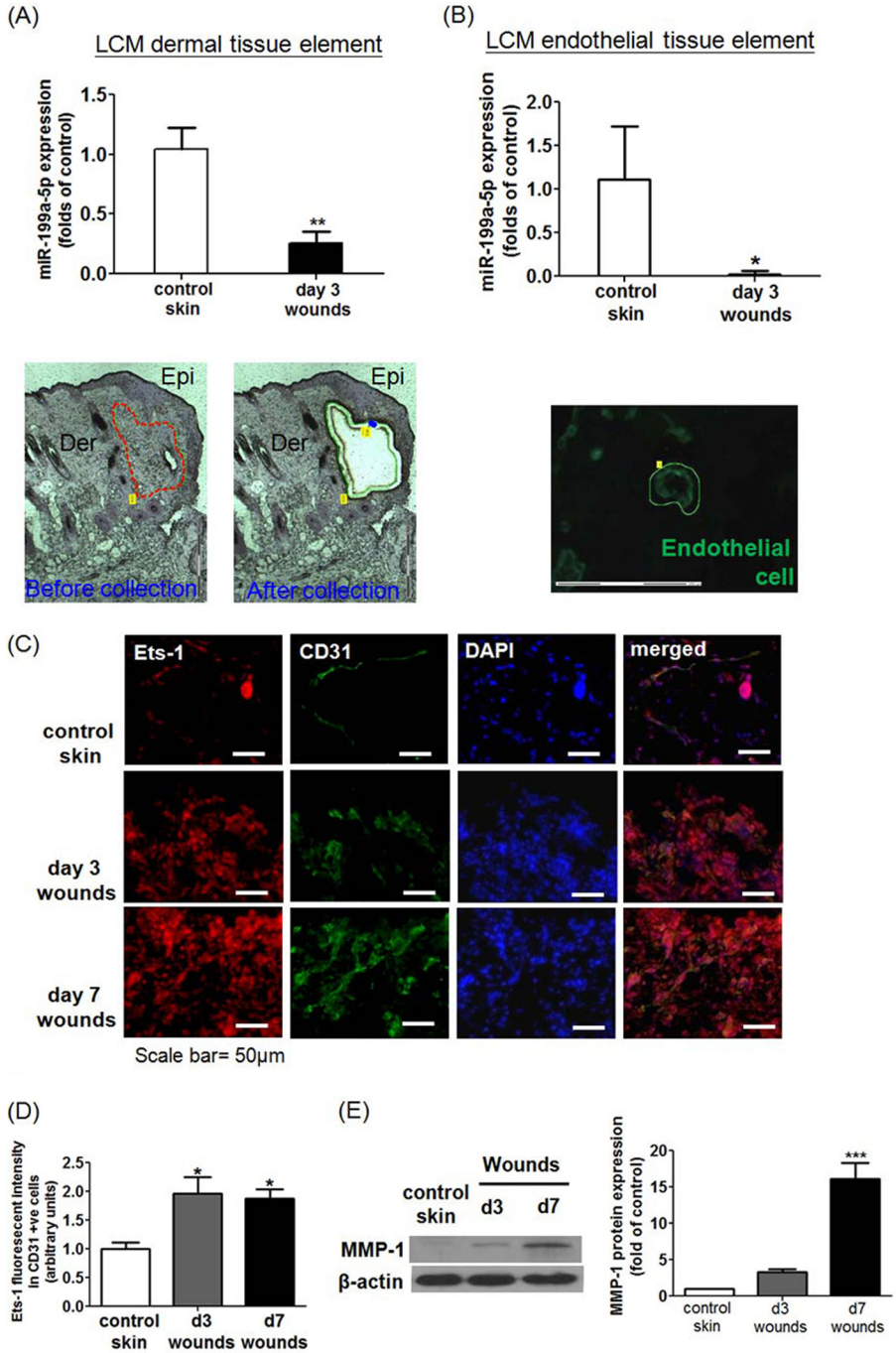

FIGURE 5. **Down-regulation of dermal and endothelial miR-199a-5p expression and induction of Ets-1 and MMP-1 in murine cutaneous wound edge tissue.** *A* and *B*, real time PCR analysis of miR-199a-5p expression in laser-captured microdissected dermis (*A*, $n = 4$) or endothelial cells (*B*, $n = 3$) from intact skin or day 3 wound edge tissues (*Epi*, epidermis; *Der*, dermis). *C*, representative diagram shows Ets-1 immunohistochemistry (*red*) in the intact skin and wound sample from days 3 and 7 postwounding ($n = 4$). Co-localization of the Ets-1 signal with endothelial marker CD31 (*green*) was achieved by co-incubation of anti-CD31 and anti-Ets-1 antibodies, counterstained with DAPI (*blue*). *D*, *bar graph* indicates quantification of Ets-1 intensity in CD31 positive cells. *E*, Western blot analysis of MMP-1 protein expression in skin and day 3 and 7 wound tissue from C57BL/6 mice. β-Actin serves as loading control. Representative blots from three independent experiments and quantification of band intensity relative to control are presented ($n = 3$). The results are the means ± S.E. *, $p < 0.05$; **, $p < 0.01$; ***, $p < 0.001$ compared with skin.

DISCUSSION

miR-199a-5p, first characterized in 2003, is derived from two genetic loci in human genome (chromosome 19 for miR-199a-1; chromosome 1 for miR-199a-2). It is well documented that inducible miR-199a-5p arrests cell proliferation and contributes to cell death (7, 8, 26, 27). Our group and others have previously reported that miR-199a-5p regulates cellular detoxifying systems by targeting multidrug resistance-associated protein 1 (6) and CD44 (12). In cardiovascular biology, although miR-199a-5p is known to play a critical role in regulating the function of cardiomyocytes (7, 8, 28–31), information on its significance in vascular biology is scanty. This study provides the first evidence demonstrating that endogenous miR-199a-5p blocks angiogenic response by targeting master transcription factor Ets-1 in endothelial cells.

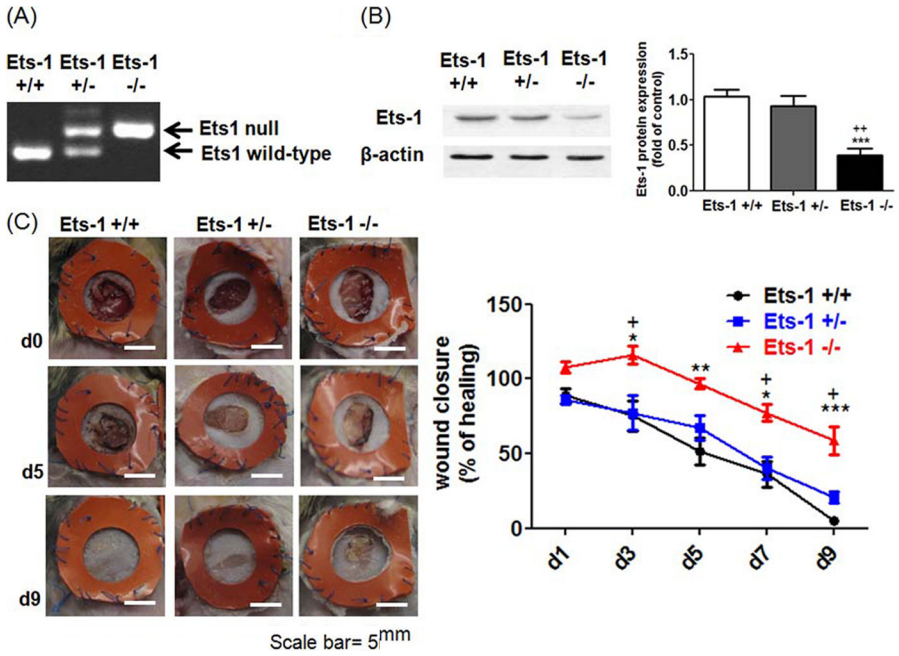

FIGURE 6. **Ets-1 knock-out mice exhibit impaired wound closure.** *A*, representative gel photo of genotyping PCR showing the presence of Ets-1 null band (250 bp) in PCR product from Ets-$1^{-/-}$ tissue. PCR product from Ets-$1^{+/-}$ mouse tissue reveals the presence of both wild type (200 bp) and null band, whereas Ets-$1^{+/+}$ mice contain only the wild type band. *B*, Western blot analysis of Ets-1 protein expression in skin tissue from Ets-$1^{+/+}$, Ets-$1^{+/-}$, and Ets-$1^{-/-}$ mice. β-Actin serves as a loading control. Representative blots from three independent experiments and quantification of band intensity relative to control are presented ($n = 4$). *C*, wound closure was monitored on day (*d*) 1, 3, 5, 7, and 9 postwounding in Ets-$1^{+/+}$, Ets-$1^{+/-}$, and Ets-$1^{-/-}$ mice by digital planimetry and was presented as a percentage of wound closure ($n = 4$). *, $p < 0.05$; **, $p < 0.01$; ***, $p < 0.001$ compared with Ets-$1^{+/+}$ mice; +, $p < 0.05$; ++, $p < 0.01$ compared with Ets-$1^{+/-}$ mice.

Ample evidence supports the notion that miRs controlling cell migration serve as endogenous regulators of angiogenesis in endothelial cells. miR-125b, for example, blocks epithelial cell migration (32, 33) and inhibits angiogenic response by targeting VE-Cadherin (34). miR-27b, a miR facilitating breast cancer cell invasiveness (35), promotes angiogenesis in endothelial cells by targeting angiostatic protein semaphorin 6A (36). miR-107, a miR down-regulated by hypoxia, attenuates cell migration (37, 38) and blocks VEGF-dependent angiogenesis by targeting hypoxia-inducing factor (HIF)-1β (39). The current study, together with findings from previous reports, reinforces the concept that miR-199a-5p not only inhibits cell migration (9, 13, 16) but also exerts potent angiostatic effect on endothelial cells by targeting a discrete subset of gene(s).

Ets-1 serves as a master transcription factor regulating angiogenic gene expression in endothelial cells including MMPs, urokinase type plasminogen activator, and vascular endothelial growth factor receptor 2 (3, 25). Induction of Ets-1 expression has been reported during tissue repair such as skin burn wounds (40), gastric ulcer (41), and aortic injury (42) aiding angiogenesis. Pro-angiogenic stimuli induce the expression of Ets-1 via transcriptional control. Moderate hypoxia, a potent angiogenic stimulus, induces Ets-1 promoter activity and Ets-1 expression via activation of HIF (43). Hydrogen peroxide, a well known pro-angiogenic stimulus (44, 45), activates nuclear factor (erythroid-derived 2)-like 2, leading to binding to antioxidant response elements and subsequent enhancement of Ets-1 promoter activity (46). Retinoic acid induces angiogenesis (47), with concomitant induction of Ets-1 transactivation (48). The findings from the current investigation, which agree with our previously published work (3), suggest an additional mechanism: Ets-1 expression is regulated through post-transcriptional modification in response to angiogenic stimulation. Indeed, miRs targeting Ets-1, namely miR-125b (49) and miR-222 (50), was also reported to serve as a potent angiostatic signal in endothelial cells (34, 51, 52), suggesting a sophisticated regulatory circuit in fine-tuning the behavior of endothelial cells in response to angiogenic signal.

In this study, we connect our *in vitro* observation to *in vivo* murine wound healing outcomes and report for the first time the involvement of miR-199a-5p-Ets-1 pathway in regulating MMP-1 expression in the context of cutaneous wound angiogenic response. Using the genetic approach, we demonstrate that the loss of Ets-1 compromises wound angiogenesis, compromises granulation tissue formation, and impairs wound closure. Intriguingly, mice with genetic deletion of Ets-1 show normal keratinocyte proliferation and differentiation (53), suggesting that the nonhealing phenotype of Ets-1 knock-out mice is likely independent of keratinocyte malfunction. We further characterized that MMP-1, which is reported to be vital in wound re-epithelialization (54), is specific to the miR-199a-5p-Ets-1 pathway. Consistent with findings from previous reports (25), Ets-1 regulates other MMP genes such as MMP-3 and MMP-9 in HMECs. However, the expression of these genes is not solely controlled by Ets-1. Instead, these genes are modulated by other transcription factors or transrepressors that might be targeted by miR-199a-5p, resulting in an off-set effect of the expression level.

A number of studies have reported the molecular mechanism of miR-199a-5p down-regulation in response to extracellular stimuli. Hypoxia induces the loss of miR-199a-5p in cardiomyocytes (7) and endothelial cells (14). Inhibition of HIF-1α

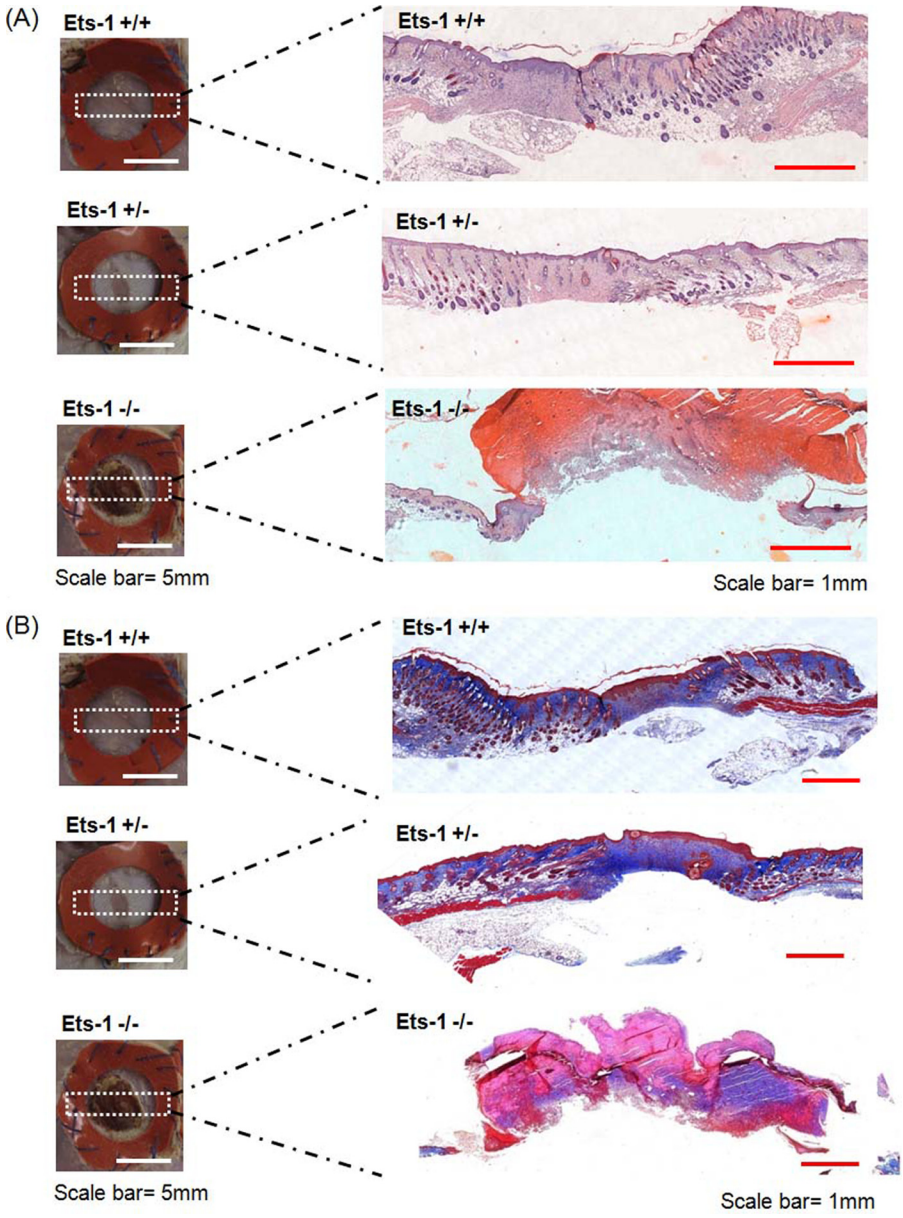

FIGURE 7. **Histological analyses of cutaneous wound edge tissue from Ets-1 knock-out mice.** Representative images of hematoxylin-eosin (*A*) and Masson trichrome staining (*B*) of d9 wound tissue from Ets-1$^{+/+}$, Ets-1$^{+/-}$, and Ets-1$^{-/-}$ mice are shown. Both hematoxylin-eosin and Masson's trichrome staining were performed on wound tissue sections obtained from three different wounds from wild type, heterozygous, and homozygous knock-out animals.

activation resulted in miR-199a-5p induction in human colon cancer cells (55). Interestingly, down-regulation of miR-199a-5p derepressed HIF-1α (7), resulting in a positive feed forward loop under modest low oxygen environment. Apart from the HIF-dependent pathway, Akt is another intracellular signal that is implicated in miR-199a-5p down-regulation. Insulin stimulation inhibits the expression of miR-199a-5p with the concomitance of Akt activation (8). Constitutively active Akt repressed miR-199a-5p expression and was associated with accumulation of miR-199a-5p target HIF-1α (8). Given the fact that activation of both HIF (56, 57) and Akt (58, 59) takes place in the early stage of skin wound healing, it is tempting to speculate that these two pathways might act simultaneously to suppress miR-199a-5p expression, resulting in derepression of Ets-1 and enabling wound angiogenesis in a MMP-1-dependent mechanism. Further investigation is required to characterize the upstream stimuli in regulating the wound-associated down-regulation of miR-199a-5p.

In summary, our results demonstrate a novel post-transcriptional control of Ets-1 expression by miR-199a-5p, and the regulation of its associated downstream mediator MMP-1. These findings reinforce the notion that miRs serve as common endogenous signals in regulating the motility of both epithelial and endothelial cells by targeting discrete set of genes. This work also provides the first evidence that wound-associated down-regulation of miR-199a-5p facilitates angiogenesis via desilencing Ets-1. Taken together, this investigation provides novel mechanistic insight explaining miR-dependent regulation of wound angiogenesis and provides the foundation of developing therapeutic intervention in treating complications of vasculopathy such as chronic nonhealing wounds.

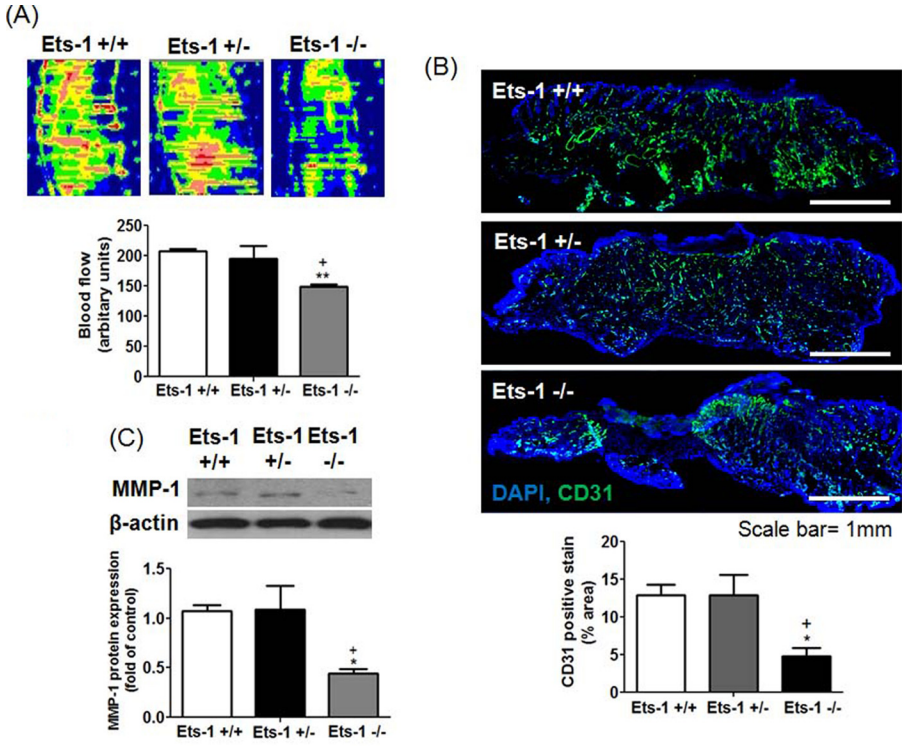

FIGURE 8. **Ets-1 knock-out mice exhibit impaired wound angiogenesis.** *A*, representative laser Doppler image of day 7 wound tissue from Ets-1$^{+/+}$, Ets-1$^{+/-}$, and Ets-1$^{-/-}$ mice. Quantification of blood flow in the wound edge area is presented as the mean ± S.E. ($n = 5$). *B*, representative images from immunostaining of CD31 from day 7 wound tissue from Ets-1$^{+/+}$, Ets-1$^{+/-}$, and Ets-1$^{-/-}$ mice. The *bar graph* represents quantification of CD31 positive area in the wound area ($n = 4$). *C*, Western blot analysis of MMP-1 protein expression in day 7 wound tissue from Ets-1$^{+/+}$, Ets-1$^{+/-}$, and Ets-1$^{-/-}$ mice. β-Actin serves as loading control. Representative blots from three independent experiments and quantification of band intensity relative to control are presented ($n = 3$). **, $p < 0.01$; *, $p < 0.05$ compared with Ets-1$^{+/+}$ mice; +, $p < 0.05$ compared with Ets-1$^{+/-}$ mice.

Acknowledgments—We thank Dr. Michael Ostrowski for providing Ets-1 cDNA clone and Ets-1 knock-out mice as generous gifts.

REFERENCES

1. Chan, Y. C., Banerjee, J., Choi, S. Y., and Sen, C. K. (2012) miR-210. The master hypoxamir. *Microcirculation* **19,** 215–223
2. Shilo, S., Roy, S., Khanna, S., and Sen, C. K. (2008) Evidence for the involvement of miRNA in redox regulated angiogenic response of human microvascular endothelial cells. *Arterioscler. Thromb. Vasc. Biol.* **28,** 471–477
3. Chan, Y. C., Khanna, S., Roy, S., and Sen, C. K. (2011) miR-200b targets Ets-1 and is down-regulated by hypoxia to induce angiogenic response of endothelial cells. *J. Biol. Chem.* **286,** 2047–2056
4. McArthur, K., Feng, B., Wu, Y., Chen, S., and Chakrabarti, S. (2011) MicroRNA-200b regulates vascular endothelial growth factor-mediated alterations in diabetic retinopathy. *Diabetes* **60,** 1314–1323
5. Chan, Y. C., Roy, S., Khanna, S., and Sen, C. K. (2012) Downregulation of endothelial microRNA-200b supports cutaneous wound angiogenesis by desilencing GATA binding protein 2 and vascular endothelial growth factor receptor 2. *Arterioscler. Thromb. Vasc. Biol.* **32,** 1372–1382
6. Park, H. A., Kubicki, N., Gnyawali, S., Chan, Y. C., Roy, S., Khanna, S., and Sen, C. K. (2011) Natural vitamin E α-tocotrienol protects against ischemic stroke by induction of multidrug resistance-associated protein 1. *Stroke* **42,** 2308–2314
7. Rane, S., He, M., Sayed, D., Vashistha, H., Malhotra, A., Sadoshima, J., Vatner, D. E., Vatner, S. F., and Abdellatif, M. (2009) Downregulation of miR-199a derepresses hypoxia-inducible factor-1α and Sirtuin 1 and recapitulates hypoxia preconditioning in cardiac myocytes. *Circ. Res.* **104,** 879–886
8. Rane, S., He, M., Sayed, D., Yan, L., Vatner, D., and Abdellatif, M. (2010) An antagonism between the AKT and beta-adrenergic signaling pathways mediated through their reciprocal effects on miR-199a-5p. *Cell Signal* **22,** 1054–1062
9. Shen, Q., Cicinnati, V. R., Zhang, X., Iacob, S., Weber, F., Sotiropoulos, G. C., Radtke, A., Lu, M., Paul, A., Gerken, G., and Beckebaum, S. (2010) Role of microRNA-199a-5p and discoidin domain receptor 1 in human hepatocellular carcinoma invasion. *Mol. Cancer* **9,** 227
10. Ueda, T., Volinia, S., Okumura, H., Shimizu, M., Taccioli, C., Rossi, S., Alder, H., Liu, C. G., Oue, N., Yasui, W., Yoshida, K., Sasaki, H., Nomura, S., Seto, Y., Kaminishi, M., Calin, G. A., and Croce, C. M. (2010) Relation between microRNA expression and progression and prognosis of gastric cancer. A microRNA expression analysis. *Lancet Oncol.* **11,** 136–146
11. Nam, E. J., Yoon, H., Kim, S. W., Kim, H., Kim, Y. T., Kim, J. H., Kim, J. W., and Kim, S. (2008) MicroRNA expression profiles in serous ovarian carcinoma. *Clin. Cancer Res.* **14,** 2690–2695
12. Cheng, W., Liu, T., Wan, X., Gao, Y., and Wang, H. (2012) MicroRNA-199a targets CD44 to suppress the tumorigenicity and multidrug resistance of ovarian cancer-initiating cells. *FEBS J* **279,** 2047–2059
13. Cheung, H. H., Davis, A. J., Lee, T. L., Pang, A. L., Nagrani, S., Rennert, O. M., and Chan, W. Y. (2011) Methylation of an intronic region regulates miR-199a in testicular tumor malignancy. *Oncogene* **30,** 3404–3415
14. Gonsalves, C. S., and Kalra, V. K. (2010) Hypoxia-mediated expression of 5-lipoxygenase-activating protein involves HIF-1α and NF-κB and microRNAs 135a and 199a-5p. *J. Immunol.* **184,** 3878–3888
15. Mizuno, S., Bogaard, H. J., Gomez-Arroyo, J., Alhussaini, A., Kraskauskas, D., Cool, C. D., and Voelkel, N. F. (2012) MicroRNA-199a-5p is associated with hypoxia inducible factor-1α expression in the lung from COPD patients. *Chest* **142,** 663–672
16. Mudduluru, G., Ceppi, P., Kumarswamy, R., Scagliotti, G. V., Papotti, M., and Allgayer, H. (2011) Regulation of Axl receptor tyrosine kinase expression by miR-34a and miR-199a/b in solid cancer. *Oncogene* **30,** 2888–2899
17. Yang, B. S., Hauser, C. A., Henkel, G., Colman, M. S., Van Beveren, C., Stacey, K. J., Hume, D. A., Maki, R. A., and Ostrowski, M. C. (1996) Ras-mediated phosphorylation of a conserved threonine residue enhances the

transactivation activities of c-Ets1 and c-Ets2. *Mol. Cell. Biol.* **16,** 538–547
18. Wong, V. W., Sorkin, M., Glotzbach, J. P., Longaker, M. T., and Gurtner, G. C. (2011) Surgical approaches to create murine models of human wound healing. *J. Biomed. Biotechnol.* **2011,** 969618
19. Biswas, S., Roy, S., Banerjee, J., Hussain, S. R., Khanna, S., Meenakshisundaram, G., Kuppusamy, P., Friedman, A., and Sen, C. K. (2010) Hypoxia inducible microRNA 210 attenuates keratinocyte proliferation and impairs closure in a murine model of ischemic wounds. *Proc. Natl. Acad. Sci. U.S.A.* **107,** 6976–6981
20. Bonta, P. I., Matlung, H. L., Vos, M., Peters, S. L., Pannekoek, H., Bakker, E. N., and de Vries, C. J. (2010) Nuclear receptor Nur77 inhibits vascular outward remodelling and reduces macrophage accumulation and matrix metalloproteinase levels. *Cardiovasc. Res.* **87,** 561–568
21. Ojha, N., Roy, S., Radtke, J., Simonetti, O., Gnyawali, S., Zweier, J. L., Kuppusamy, P., and Sen, C. K. (2008) Characterization of the structural and functional changes in the myocardium following focal ischemia-reperfusion injury. *Am. J. Physiol. Heart Circ. Physiol.* **294,** H2435–H2443
22. Hsu, P. W., Lin, L. Z., Hsu, S. D., Hsu, J. B., and Huang, H. D. (2007) ViTa. Prediction of host microRNAs targets on viruses. *Nucleic Acids Res.* **35,** D381–385
23. Krek, A., Grün, D., Poy, M. N., Wolf, R., Rosenberg, L., Epstein, E. J., MacMenamin, P., da Piedade, I., Gunsalus, K. C., Stoffel, M., and Rajewsky, N. (2005) Combinatorial microRNA target predictions. *Nat. Genet.* **37,** 495–500
24. Wang, X. (2008) miRDB. A microRNA target prediction and functional annotation database with a wiki interface. *RNA* **14,** 1012–1017
25. Dittmer, J. (2003) The biology of the Ets1 proto-oncogene. *Mol. Cancer* **2,** 29–49
26. Jia, X. Q., Cheng, H. Q., Qian, X., Bian, C. X., Shi, Z. M., Zhang, J. P., Jiang, B. H., and Feng, Z. Q. (2012) Lentivirus-mediated overexpression of microRNA-199a inhibits cell proliferation of human hepatocellular carcinoma. *Cell Biochem. Biophys.* **62,** 237–244
27. Tsukigi, M., Bilim, V., Yuuki, K., Ugolkov, A., Naito, S., Nagaoka, A., Kato, T., Motoyama, T., and Tomita, Y. (2012) Re-expression of miR-199a suppresses renal cancer cell proliferation and survival by targeting GSK-3β. *Cancer Lett.* **315,** 189–197
28. Song, X. W., Li, Q., Lin, L., Wang, X. C., Li, D. F., Wang, G. K., Ren, A. J., Wang, Y. R., Qin, Y. W., Yuan, W. J., and Jing, Q. (2010) MicroRNAs are dynamically regulated in hypertrophic hearts, and miR-199a is essential for the maintenance of cell size in cardiomyocytes. *J. Cell. Physiol.* **225,** 437–443
29. Salloum, F. N., Yin, C., and Kukreja, R. C. (2010) Role of microRNAs in cardiac preconditioning. *J. Cardiovasc. Pharmacol.* **56,** 581–588
30. Ye, Y., Perez-Polo, J. R., Qian, J., and Birnbaum, Y. (2011) The role of microRNA in modulating myocardial ischemia-reperfusion injury. *Physiol. Genomics* **43,** 534–542
31. Haghikia, A., Missol-Kolka, E., Tsikas, D., Venturini, L., Brundiers, S., Castoldi, M., Muckenthaler, M. U., Eder, M., Stapel, B., Thum, T., Petrasch-Parwez, E., Drexler, H., Hilfiker-Kleiner, D., and Scherr, M. (2011) Signal transducer and activator of transcription 3-mediated regulation of miR-199a-5p links cardiomyocyte and endothelial cell function in the heart. A key role for ubiquitin-conjugating enzymes. *Eur. Heart J.* **32,** 1287–1297
32. Liang, L., Wong, C. M., Ying, Q., Fan, D. N., Huang, S., Ding, J., Yao, J., Yan, M., Li, J., Yao, M., Ng, I. O., and He, X. (2010) MicroRNA-125b suppressesed human liver cancer cell proliferation and metastasis by directly targeting oncogene LIN28B2. *Hepatology* **52,** 1731–1740
33. Liu, L. H., Li, H., Li, J. P., Zhong, H., Zhang, H. C., Chen, J., and Xiao, T. (2011) miR-125b suppresses the proliferation and migration of osteosarcoma cells through down-regulation of STAT3. *Biochem. Biophys. Res. Commun.* **416,** 31–38
34. Muramatsu, F., Kidoya, H., Naito, H., Sakimoto, S., and Takakura, N. (2012) MicroRNA-125b inhibits tube formation of blood vessels through translational suppression of VE-cadherin. *Oncogene*, in press
35. Wang, Y., Rathinam, R., Walch, A., and Alahari, S. K. (2009) ST14 (suppression of tumorigenicity 14) gene is a target for miR-27b, and the inhibitory effect of ST14 on cell growth is independent of miR-27b regulation. *J. Biol. Chem.* **284,** 23094–23106
36. Urbich, C., Kaluza, D., Frömel, T., Knau, A., Bennewitz, K., Boon, R. A., Bonauer, A., Doebele, C., Boeckel, J. N., Hergenreider, E., Zeiher, A. M., Kroll, J., Fleming, I., and Dimmeler, S. (2012) MicroRNA-27a/b controls endothelial cell repulsion and angiogenesis by targeting semaphorin 6A. *Blood* **119,** 1607–1616
37. Li, X., Zhang, Y., Shi, Y., Dong, G., Liang, J., Han, Y., Wang, X., Zhao, Q., Ding, J., Wu, K., and Fan, D. (2011) MicroRNA-107, an oncogene microRNA that regulates tumour invasion and metastasis by targeting DICER1 in gastric cancer. *J. Cell Mol. Med.* **15,** 1887–1895
38. Moncini, S., Salvi, A., Zuccotti, P., Viero, G., Quattrone, A., Barlati, S., De Petro, G., Venturin, M., and Riva, P. (2011) The role of miR-103 and miR-107 in regulation of CDK5R1 expression and in cellular migration. *PLoS One* **6,** e20038
39. Yamakuchi, M., Lotterman, C. D., Bao, C., Hruban, R. H., Karim, B., Mendell, J. T., Huso, D., and Lowenstein, C. J. (2010) P53-induced microRNA-107 inhibits HIF-1 and tumor angiogenesis. *Proc. Natl. Acad. Sci. U.S.A.* **107,** 6334–6339
40. Wernert, N., Raes, M. B., Lassalle, P., Dehouck, M. P., Gosselin, B., Vandenbunder, B., and Stehelin, D. (1992) c-ets1 proto-oncogene is a transcription factor expressed in endothelial cells during tumor vascularization and other forms of angiogenesis in humans. *Am. J. Pathol.* **140,** 119–127
41. Ito, M., Nakayama, T., Naito, S., Matsuu, M., Shichijo, K., and Sekine, I. (1998) Expression of Ets-1 transcription factor in relation to angiogenesis in the healing process of gastric ulcer. *Biochem. Biophys. Res. Commun.* **246,** 123–127
42. Tanaka, K., Oda, N., Iwasaka, C., Abe, M., and Sato, Y. (1998) Induction of Ets-1 in endothelial cells during reendothelialization after denuding injury. *J. Cell. Physiol.* **176,** 235–244
43. Oikawa, M., Abe, M., Kurosawa, H., Hida, W., Shirato, K., and Sato, Y. (2001) Hypoxia induces transcription factor ETS-1 via the activity of hypoxia-inducible factor-1. *Biochem. Biophys. Res. Commun.* **289,** 39–43
44. Sen, C. K., Khanna, S., Babior, B. M., Hunt, T. K., Ellison, E. C., and Roy, S. (2002) Oxidant-induced vascular endothelial growth factor expression in human keratinocytes and cutaneous wound healing. *J. Biol. Chem.* **277,** 33284–33290
45. Roy, S., Khanna, S., Nallu, K., Hunt, T. K., and Sen, C. K. (2006) Dermal wound healing is subject to redox control. *Mol. Ther.* **13,** 211–220
46. Wilson, L. A., Gemin, A., Espiritu, R., and Singh, G. (2005) Ets-1 is transcriptionally up-regulated by H2O2 via an antioxidant response element. *FASEB J.* **19,** 2085–2087
47. Saito, A., Sugawara, A., Uruno, A., Kudo, M., Kagechika, H., Sato, Y., Owada, Y., Kondo, H., Sato, M., Kurabayashi, M., Imaizumi, M., Tsuchiya, S., and Ito, S. (2007) All-*trans*-retinoic acid induces in vitro angiogenesis via retinoic acid receptor. Possible involvement of paracrine effects of endogenous vascular endothelial growth factor signaling. *Endocrinology* **148,** 1412–1423
48. Raouf, A., Li, V., Kola, I., Watson, D. K., and Seth, A. (2000) The Ets1 proto-oncogene is upregulated by retinoic acid. Characterization of a functional retinoic acid response element in the Ets1 promoter. *Oncogene* **19,** 1969–1974
49. Zhang, Y., Yan, L. X., Wu, Q. N., Du, Z. M., Chen, J., Liao, D. Z., Huang, M. Y., Hou, J. H., Wu, Q. L., Zeng, M. S., Huang, W. L., Zeng, Y. X., and Shao, J. Y. (2011) miR-125b is methylated and functions as a tumor suppressor by regulating the ETS1 proto-oncogene in human invasive breast cancer. *Cancer Res.* **71,** 3552–3562
50. Mattia, G., Errico, M. C., Felicetti, F., Petrini, M., Bottero, L., Tomasello, L., Romania, P., Boe, A., Segnalini, P., Di Virgilio, A., Colombo, M. P., and Carè, A. (2011) Constitutive activation of the ETS-1-miR-222 circuitry in metastatic melanoma. *Pigment Cell Melanoma Res.* **24,** 953–965
51. Poliseno, L., Tuccoli, A., Mariani, L., Evangelista, M., Citti, L., Woods, K., Mercatanti, A., Hammond, S., and Rainaldi, G. (2006) MicroRNAs modulate the angiogenic properties of HUVECs. *Blood* **108,** 3068–3071
52. Suárez, Y., Fernández-Hernando, C., Pober, J. S., and Sessa, W. C. (2007) Dicer dependent microRNAs regulate gene expression and functions in human endothelial cells. *Circ. Res.* **100,** 1164–1173
53. Nagarajan, P., Parikh, N., Garrett-Sinha, L. A., and Sinha, S. (2009) Ets1 induces dysplastic changes when expressed in terminally-differentiating

squamous epidermal cells. *PLoS One* **4,** e4179
54. Stevens, L. J., and Page-McCaw, A. (2012) A secreted MMP is required for reepithelialization during wound healing. *Mol. Biol. Cell* **23,** 1068–1079
55. Kang, S. G., Lee, W. H., Lee, Y. H., Lee, Y. S., and Kim, S. G. (2012) Hypoxia-inducible factor-1α inhibition by a pyrrolopyrazine metabolite of oltipraz as a consequence of microRNAs 199a-5p and 20a induction. *Carcinogenesis* **33,** 661–669
56. Elson, D. A., Ryan, H. E., Snow, J. W., Johnson, R., and Arbeit, J. M. (2000) Coordinate up-regulation of hypoxia inducible factor (HIF)-1α and HIF-1 target genes during multi-stage epidermal carcinogenesis and wound healing. *Cancer Res.* **60,** 6189–6195
57. Botusan, I. R., Sunkari, V. G., Savu, O., Catrina, A. I., Grünler, J., Lindberg, S., Pereira, T., Ylä-Herttuala, S., Poellinger, L., Brismar, K., and Catrina, S. B. (2008) Stabilization of HIF-1α is critical to improve wound healing in diabetic mice. *Proc. Natl. Acad. Sci. U.S.A.* **105,** 19426–19431
58. Squarize, C. H., Castilho, R. M., Bugge, T. H., and Gutkind, J. S. (2010) Accelerated wound healing by mTOR activation in genetically defined mouse models. *PLoS One* **5,** e10643
59. Lima, M. H., Caricilli, A. M., de Abreu, L. L., Araújo, E. P., Pelegrinelli, F. F., Thirone, A. C., Tsukumo, D. M., Pessoa, A. F., dos Santos, M. F., de Moraes, M. A., Carvalheira, J. B., Velloso, L. A., and Saad, M. J. (2012) Topical insulin accelerates wound healing in diabetes by enhancing the AKT and ERK pathways. A double-blind placebo-controlled clinical trial. *PLoS One* **7,** e36974

The MicroRNA miR-199a-5p Down-regulation Switches on Wound Angiogenesis by Derepressing the *v-ets* Erythroblastosis Virus E26 Oncogene Homolog 1-Matrix Metalloproteinase-1 Pathway

Yuk Cheung Chan, Sashwati Roy, Yue Huang, Savita Khanna and Chandan K. Sen

J. Biol. Chem. 2012, 287:41032-41043.
doi: 10.1074/jbc.M112.413294 originally published online October 11, 2012
